ELSEVIER

Journal of Power Sources 88 (2000) 53–70

JOURNAL OF POWER SOURCES

www.elsevier.com/locate/jpowsour

Research update from European Advanced Lead–Acid Battery Consortium

A. Cooper *

European Advanced Lead–Acid Battery Consortium (EEIG), 42 Weymouth Street, W1N 3LQ London, UK

Received 5 August 1999; accepted 10 October 1999

Abstract

In July 1997, the European members of the Advanced Lead–Acid Battery Consortium were awarded a second Brite-EuRam contract for research on lead–acid batteries for electric vehicles (EVs). This Project, entitled 'Strategies for the further improvement of performance and life of lead–acid batteries for electric vehicle applications', commenced at the beginning of January 1998, is costing some US$4 million, and is scheduled to run for 3 years. The Project is divided into three principal tasks. The first is concentrating on separator design and compression in order to improve cycle-life. In the second task, attempts are being made to improve the specific energy of tubular-plate designs, which traditionally have good life characteristics in traction applications. In addition, work is being carried out to determine the effects of rapid-charging techniques on this type of battery design. The third task is attempting to improve the performance of negative plates by seeking improved expanders. The Project has now reached its mid-point. This paper describes the work in progress and discusses some of the results achieved to date and their implication for the future of the research programme.

Keywords: Compression; Electric vehicles; Expanders; Fast charging; Separators; Tubular plates; Valve-regulated lead–acid batteries

1. Background

The present Brite-EuRam project is designed to follow, and build upon, the results achieved in the previous Project BE 7297. Certain key outcomes of that research can be stated as follows.

- At the high rates of discharge experienced in electric vehicle (EV) applications, active-material utilisation in lead–acid batteries is limited by acid availability rather than by paste conductivity. Thus, there is limited scope for improvements to specific energy by additives to the positive active mass (PAM).
- Principal factors in the improvement of the cycle-life of valve-regulated lead–acid (VRLA) batteries have been shown to be: compression of the active mass by the separator; construction of the absorptive glass mat separator; nature of the charge regime employed to recharge the battery after use.
- It has been possible to enhance considerably the properties of the grid alloys (strength and corrosion resistance) by additions of tin and silver.

Work elsewhere has shown that rapid charging techniques, in addition to radically reducing recharging times, can also improve the cycle-life of flat-plate batteries, apparently by modifying the structure of the active material [1]. Such techniques can, however, result in elevated temperatures in the battery and this can be detrimental to the life of negative plates. Under certain test regimes for EV batteries, it has been further demonstrated that the negative plate can fail under the influence of repeated, and prolonged, high-rate discharge pulses [2].

Accordingly, the work in the new Project is focused in three areas, as follows.

- The study of separator compression across the plate stack as a whole, in order to determine the reasons for the early initial loss of capacity experienced in these designs. Several different separator designs will be studied to overcome problems of acid stratification and relaxation of compression during service.
- The improvement of specific energy and life of lead–acid batteries by the development of lightweight tubular designs using the high-strength, corrosion-resistant

* Tel.: +44-171-499-8422; fax: +44-171-493-1555.
E-mail address: acatcorfe@aol.com (A. Cooper).

0378-7753/00/$ - see front matter
PII: S0378-7753(99)00510-8

alloys mentioned above. In this type of battery, the positive active-material is constrained between the alloy spine and a porous fabric gauntlet and thus reduces opportunities for paste shedding or softening during cycling. Operating this type of battery under compression, in an AGM design, will help to maintain electronic conductivity within the active material, especially with the lower paste densities required for higher active-material utilisation. Rapid charging techniques will also be tried on these designs.

- The mechanism of the degradation of the negative plate will be studied under conditions of EV service and, following this, work will be carried out to develop improved expanders for maintenance of the required open structure in the negative active mass (NAM).

The work is expected to result in further improvements in the cycle-life and the specific energy of the lead–acid battery and a consequent reduction in running costs. This will, in turn, make the performance and cost of EVs more attractive and, hence, will improve their marketability. This will be done without detriment to the current inherent good recycling of the lead–acid battery.

2. Project structure and participants

The Project is divided into three principal tasks, which are further divided into smaller sub-tasks. These are listed below, together with the names of the contractors responsible for the work.

2.1. Task 1: Separator design and compression

(a) Study of the effects of compressive forces applied to the plate stack, using various AGM separator designs, on the cycle-life of VRLA batteries. Contractors: Oldham France, Amer-Sil, Hollingsworth and Vose (H&V), University of Kassel.
(b) Evaluation of a novel type of separator on the performance and life of VRLA batteries. Contractors: ZSW, Daramic, Sonnenschein.

2.2. Task 2: Optimising specific energy and performance of VRLA batteries utilising novel, lightweight, tubular designs and high-rate pulse charging techniques

(a) Construction and testing of optimised tubular and strap grid tubular designs with thin plates. Contractors: CMP Batteries, CLEPS, ZSW.
(b) Study of the influence of pulse-charging techniques on the specific energy, life and charge time of advanced tubular designs. Contractors: ZSW, Digatron, CMP Batteries.

2.3. Task 3. Improvements in negative-plate performance

(a) Investigations into the degradation of the performance of the negative plate arising from high-rate discharge. Contractor: CLEPS.
(b) Search for improved or synthetic expander materials for the negative plate. Contractors: Tudor Spain, Politecnico di Torino.
(c) Improvement in the performance of the NAM through better expanders. Contractor: Tudor Spain.

The Project started on 1 January 1998 and is scheduled to run for 3 years, with the three tasks running concurrently.

3. Project progress

3.1. Task 1(a): Separator design and compression

The aim of the work is to characterise the range of compressive forces that can be achieved with AGM, or modified AGM, separators. By using realistic assembly techniques, it is intended to establish the optimum compressive forces to be applied to the plate stack for the different separator types in order to extend cycle-life and to try to prevent the frequently observed early loss of capacity.

The main sub-tasks in this study are:

1(a) 1. An in-depth separator characterisation.
1(a) 2. Electrochemical studies to investigate the active material/separator relationship.
1(a) 3. Separator selection, followed by test battery assembly.
1(a) 4. Cycle-life and stratification testing of practical VRLA batteries.

As the work sets out to build upon the knowledge gained from the programme of work carried out in task 6 of BE 7297, the same battery type and cycle test regime are being used in the current work. The results of this programme will be compared with the results obtained with the task 6 AGM separator containing 75% fine fibre.

Amer-Sil has developed two novel types of separator for incorporation into the test programme. The first is a sandwich separator with the inner component made up of a special, highly porous membrane surrounded by AGM composed of 100% fine fibres. The second is made up of a multi-layered AGM separator with a layer of 100% fine fibres contacting the electrodes and an inner part with a coarser fibre structure. These separators have been fully characterised and were sent to Oldham France for building into test cells in the fourth quarter of 1998.

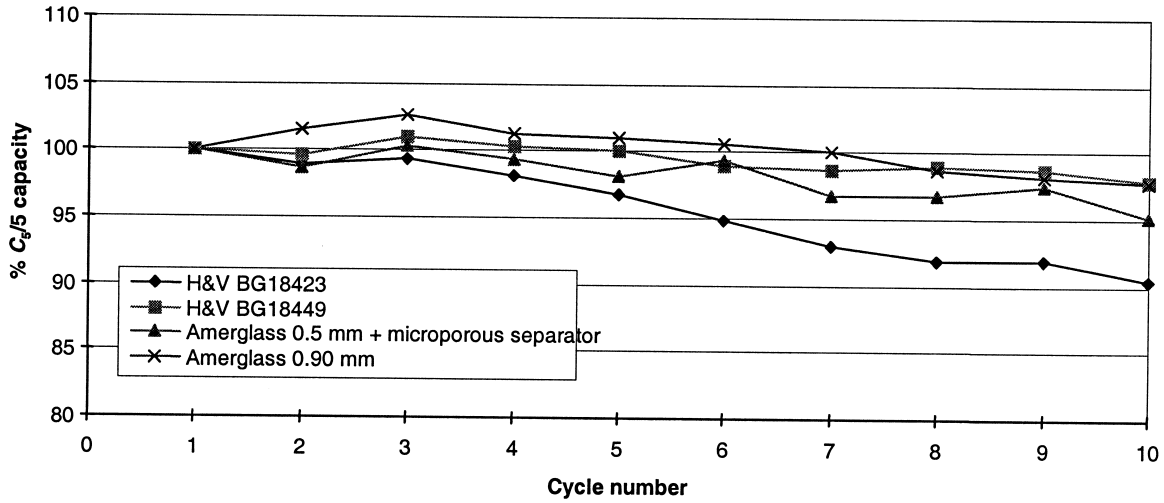

Fig. 1. Evolution of the $C_5/5$ capacity for different separator types.

At H&V, at the outset of the programme, existing separator grades were reviewed for a possible match to requirements. In addition, alternative materials were sampled and screened using 200-g m^{-2} handsheets. After evaluation, selection was made of the best base materials for use in the chosen separator types and raw material purchase was effected. Manufacturing trials were then carried out followed by a re-test of the finished product for suitability. In the end, two different separator types have been developed; these are essentially blends of AGM and organic fibres. The materials have been characterised prior to delivery to Oldham France for building into the test batteries. This work was completed during the first quarter of 1999, together with initial battery performance tests. Twelve cells of each type have been manufactured (nominal capacity 120 A h). The construction details are as follows.

Amerglass 0.5-mm separator and micro-porous separator. Each positive and negative plate is wrapped in an Amerglass 0.5-mm separator. The micro-porous separator is put between the positive and negative plate and thus, there are 48 layers of Amerglass separator and 24 layers of micro-porous separator per cell. Compression achieved on the dry separator is above 50 kPa. It should be noted that there is no layer of separator next to the container wall for the end negative plate.

Amerglass 0.9-mm separator. Each positive and negative plate is wrapped by the separator so that there are 48 layers of separator per cell. The compression achieved is about 30 kPa.

H&V type BG18423 separator. Only the positive plate is wrapped by the separator so there are 24 layers of separator per cell. Compression achieved on the dry separator is in the range 52–80 kPa.

H&V type BG 18449 separator. Similar in assembly to the type above. Compression achieved on the dry separator is about 80 kPa.

All the cells achieved the rated capacity but the Amer-Sil 0.5-mm/micro-porous membrane separator exhibited the highest scatter of capacity (6.9%). The other three types were within a range of 3.5%. The cells were subjected to initial performance and stratification tests as previously described [3]. Fig. 1 shows the evolution of capacity of the cells with the four different separator types over the first 10 cycles. Tables 1 and 2 summarise the stratification results for the Amer-Sil and H&V separators. The former show a much higher degree of stratification and this may be the result of the lower levels of compression applied to the separator. Six cells with each separator type are now being subjected to cycling tests at Amer-Sil and H&V.

Electrochemical studies are being carried out at the University of Kassel and some of these involve the mea-

Table 1
Stratification results for Amer-Sil separators

Separator type	Cell no.	Average stratification (points)	Average acid relative density
Amerglass 0.5 mm	27	122	1.285
+Micro-porous	28	125	1.285
separator			
Amerglass 0.9 mm	40	111	1.291
	43	121	1.289

Table 2
Stratification results for H&V separators

Separator type	Cell no.	Average stratification (points)	Average acid relative density
BG 18423	7	56	1.290
	8	56	1.290
BG 18449	14	68	1.281
	18	58	1.285

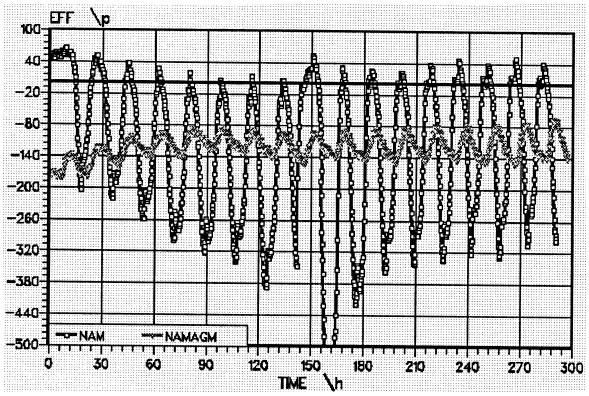

Fig. 2. Cycling of negative active-material with and without AGM.

surement of the forces evolved by the active material during cycling together with changes in the resistance. These are performed with a special cell developed at Kassel and used to study the behaviour of positive active-material in previous work (Project BE 7297). In the present Project, the behaviour of the negative active-material is being studied, as well as that of both of the active materials in conjunction with the various separator types.

In Study 1, the mechanical and electrical properties of the NAM alone have been studied. Results have shown that the NAM behaves quite differently to that of the PAM. The latter expands during formation whereas the NAM shrinks. Also, the solid-state resistance of the NAM is very small and changes relatively little during cycling.

In Study 2, a piece of separator was inserted between a rod electrode and either the NAM or PAM and the development of the forces during cycling is measured. The behaviour of the positive and negative active material is presented in Figs. 2 and 3, respectively, during cycling both in the presence of, and in the absence of, separator. It can be seen that the AGM separator tends to absorb the forces exerted by the active material.

In a further study, a special piece of equipment has been developed to measure the oxygen transport through the separator as well as its electrical resistance. This is illustrated in Fig. 4. It consists of a Plexiglass holder with

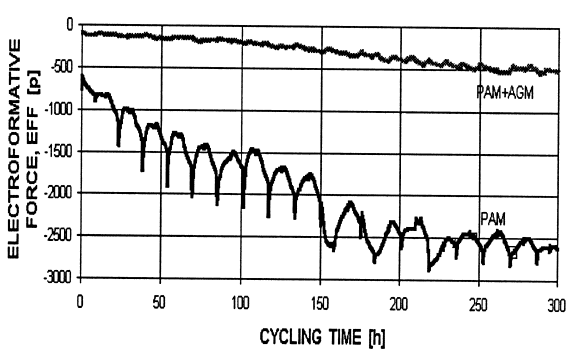

Fig. 3. Cycling of positive active-material with and without AGM.

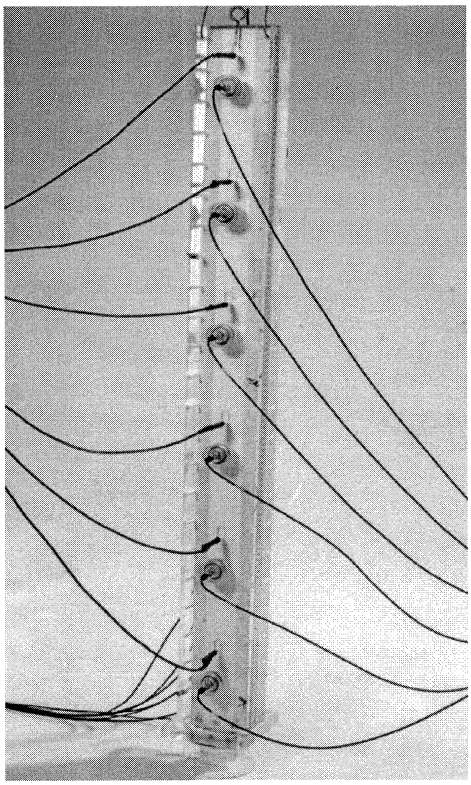

Fig. 4. Apparatus for measuring oxygen transport and separator resistance.

a separator strip held inside and compressed in a controlled fashion over its whole length. The unit is fitted with oxygen-emitting and oxygen-consuming electrochemical cells and also electrodes for measuring the resistance. The work on the rig is at a preliminary stage.

3.2. Task 1(b): Evaluation of a novel type of separator (the acid-jellifying separator, AJS) on the performance and life of VRLA batteries

The aim of the task is to manufacture, test and optimise a novel type of separator — the AJS — which is able to effect compression on the electrodes and to avoid acid stratification, in order to improve the performance and the cycle-life of VRLA batteries in comparison with conventional design options. The work programme is as follows.

- Manufacture of samples of the novel AJS separator.
- Characterisation of the AJS outside the battery.
- Design and manufacture of test cells with AJS, AGM and gel separators.
- Testing of cells.
- Optimisation of AJS, manufacture and characterisation of new samples.
- Design and manufacture of test cells with the optimised AJS.
- Testing of cells with optimised AJS.

- Manufacture of batteries with AGM, the most promising AJS and gel.
- Cycling tests of the battery with the most promising AJS in comparison with AGM and gel.

Samples of the new AJS separator have been produced at Daramic and have been characterised outside the battery, both at Daramic and ZSW. Table 3 shows how the properties of the AJS compare with typical AGM separator material.

The dependence of the thickness of the AJS separator on compression is presented in Fig. 5 for a pressure range, which could be encountered on assembly, or after expansion of the active material in a situation where the battery case does not deform. While AGM experiences about 30% deformation in a dry state under a pressure of 20 to 30 kPa, depending on the origin of the separator, AJS shows only about 0.1% deformation in this pressure range. Such a characteristic means that the room for expansion of the positive active material will be restrained through the presence of the AJS. As an additional advantage, AJS expands when wetted, in complete contrast to AGM.

Valve regulated cells, in a size of 48 A h, were built at Sonnenschein with AJS, AGM and gel as the separation and electrolyte immobilisation system. The gel cells contained phosphoric acid and the AJS variants were built with and without phosphoric acid. In addition, the optimum saturation rate for the new AJS separator, and its influence on the capacity of the cells, were investigated at Sonnenschein.

Cells with AJS, AGM and gel manufactured by Sonnenschein have been delivered to ZSW. At ZSW, these cells were assessed for their electrical performance under different discharge conditions. The dependence of capacity on discharge current at room temperature is given in Fig. 6.

Table 3
Comparison of AJS and AGM separator properties

Property	AJS	AGM
Thickness (mm)	1.2	1.85 (at 1kPa)
Electrical resistance ($m\Omega$ cm^2)	110	68
Acid absorption (1 mm thickness) ($g\ m^{-3}$)	980	1100
Porosity (%)	81	92
Pore size (μm)	0.2	13
Elongation (%)	70	3–4
Thickness decrease (100 kPa) (%)	<1	45
Acid shrinkage (%)	$+1$	0.5
Acid stratification	very slow	six times faster
Drainage	no drainage within 7 days	high drainage after 7 days

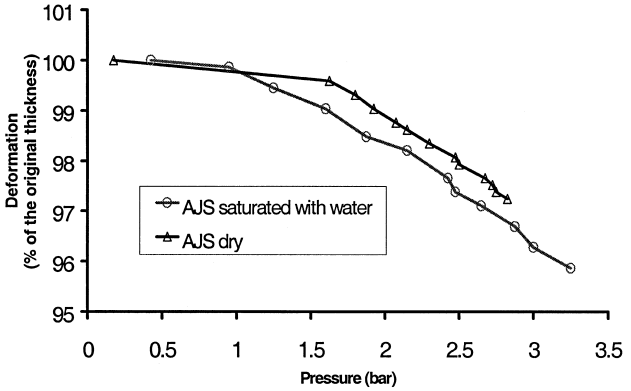

Fig. 5. Compressibility of AJS in wet and dry state.

Comparing the cells with AGM and with AJS (without phosphoric acid), a better capacity was obtained with the AJS separator although the performance of the AGM cell might have been improved if a higher saturation rate than 90% had been chosen. The presence of phosphoric acid in the electrolyte in other AJS variants lowers the capacity by around 10%. The gel cell has a similar $C_5/5$ capacity to the AJS with the phosphoric acid but is worse at the higher rates. Other tests have shown that the low-temperature performance of AJS without phosphoric acid is also better than the other systems. More surprisingly, a lower internal resistance has been found for the AJS system and a higher specific power.

Cycling tests for these cells have been started with different initial compression forces applied to the cells. The different variants selected are shown in Table 4. The development of the capacity, the charge factor and the compressive force on the battery container were studied during discharge–charge and during cycling. The evolution of the $C_2/2$ capacity is shown in Fig. 7. The initial differences in capacity were less than 10%, but the capacity of the gel cell decreased rapidly and thus the charge regime was changed at cycle 47. This resulted in an increase in the previously low charge factor from 1.015 to 1.04 and the capacity increased dramatically. Thus, because the gel cell has a different charging regime, which yields a different capacity behaviour, it is difficult to make any direct comparison with the other systems. Nevertheless, when considering the AGM and AJS systems, some really encouraging results have been obtained. The cells have performed over 250 cycles and the AJS system is performing well, particularly when placed under higher initial compression or in the presence of phosphoric acid.

The development of the force as with cycle number for the different separation systems and different initial applied pressures is given in Fig. 8. The force was measured

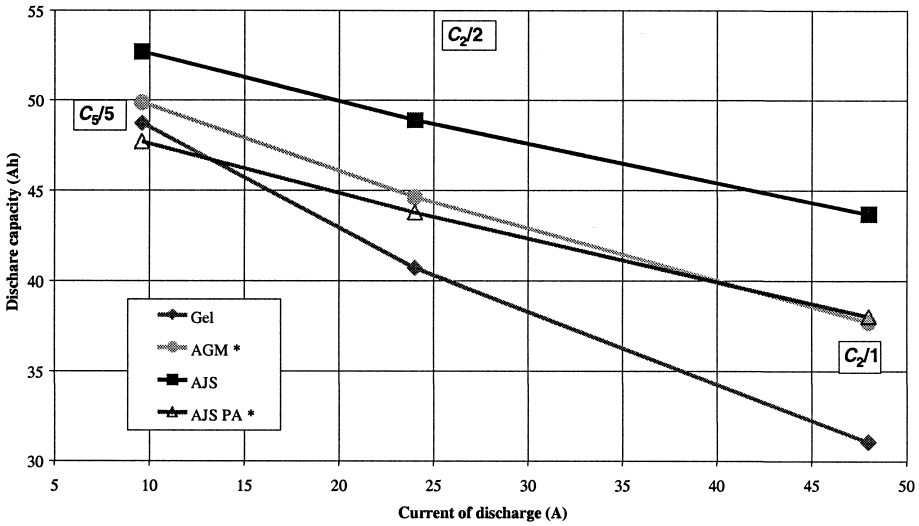

Fig. 6. Capacity dependence on discharge current at room temperature.

for each second $C_5/5$ capacity test after each series of 25 $C_2/2$ cycles at the end of discharge. That way, there would be the lowest possible superimposition of force due to gas evolution. A decrease in force from the very beginning was observed with the AJS system with phosphoric acid, the AJS without the acid at high compression (80 kPa), and the AGM system. Later, the compressive force increases slowly for all systems except the gel system. There are two levels of compressive force, one in the range of 30–40 kPa and the other in the range of 60–70 kPa. For the AJS cell with springs, it is assumed that the force stays in the range of the initial compression of 80 kPa.

The general tendency is for the compressive force to increase with cycle number. This can be explained by expansion of the PAM, which dominates in comparison with contraction of the NAM. For the gel system (for which the compressive force stays almost constant with cycling), the expansion of the active mass will not lead directly to an increase in force because there is space between the ribs of the separator. An increase in external force can be measured only via the ribs of the separator or after the space between the ribs is filled. The beneficial effect of the high compression on capacity becomes visible after approximately 170 cycles. At this stage, however, the phosphoric acid appears to be more efficient for the stabilisation of capacity than the higher compression.

Measurements have also been carried out in order to measure the recombination rate of the AJS system. This system has a lower recombination rate than its AGM counterpart but such behaviour must not necessarily be considered to be a drawback. In combination with a suitable charge regime, which prevents heavy overcharge, a low recombination rate could be acceptable and would result in an improved energy efficiency.

3.3. Task 2(a): Design, construction and testing of optimised tubular and strap tubular batteries with thin plates

Although lead–acid batteries with tubular positive plates have long cycle-lives, the high-rate performance required in EV applications has been limited by the impact of relatively large plate couple pitch on impedance and plate current density. Performance improvements are being pursued through the development of thin, tubular, positive-plate technologies.

Table 4
Variants for comparative cycling test of AGM, gel and AJS batteries

Separation	H_3PO_4	Compression	Distance
AGM	No	25% compression of separator (i.e., about 30 kPa)	Cell is compressed until nominal case thickness is reached. This distance is kept constant.
Gel	Yes	No compression	Cell is compressed until nominal case thickness is reached and this distance is then kept constant.
AJS	Yes	30 kPa initial pressure	Cell is compressed with 30 kPa and distance is then held constant.
AJS	No	30 kPa initial pressure	Cell is compressed with 30 kPa and distance is then kept constant.
AJS	No	80 kPa initial pressure	Cell is compressed with 80 kPa and distance is then kept constant.
AJS	No	80 kPa constant pressure on cell case through springs	Distance is free to change under constant compression applied by springs.

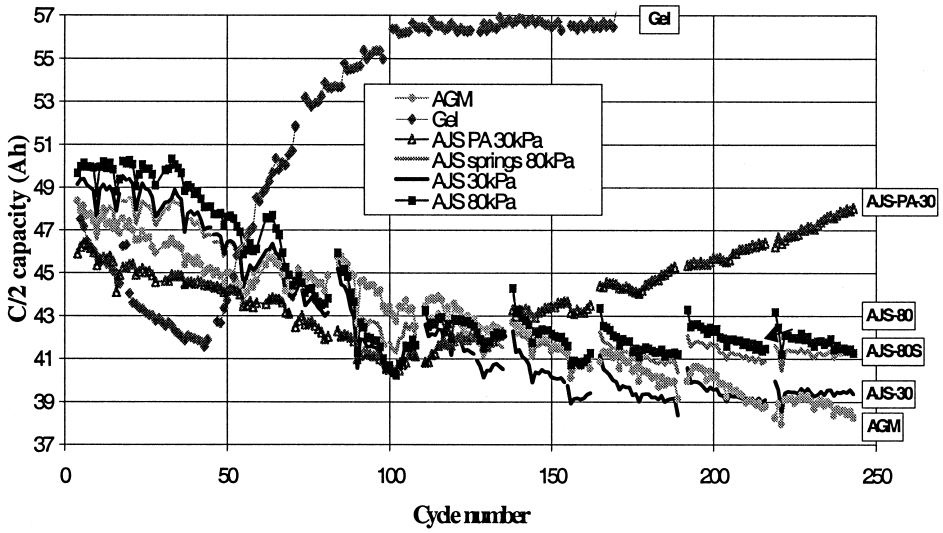

Fig. 7. Evolution of $C_2/2$ capacity with cycling for the different separator variants.

Work at CMP Batteries pursues the extension of the commercial development of progressively thinner plates, in flooded electrolyte and valve-regulated products, by using pressure die-cast spines. Positive-plate utilisation will be increased by reducing the grid mass and by adopting alloys with improved corrosion resistance, creep strength and resistance to the development of high impedance at the spine/active-material interface. The objectives of the task are as follows.

- To design, within advanced material and processing constraints, thin tubular and strap-grid positive lead–acid battery plates, which are optimised for positive-plate utilisation.
- Consider alternative approaches and develop negative plates of optimised utilisation.
- Refine and design cell components, balanced for EV duty, through testing the influences of design and process variables on battery performance.
- Design and build a thin tubular positive plate for EV batteries.
- Demonstrate sustained performance of the optimised design in cycling tests.

In the initial design, a more ambitious reduction in plate thickness was adopted in order to reduce cell impedance for EV duty. The two basic designs of cell reflected one and two extra plate couples relative to the proposed com-

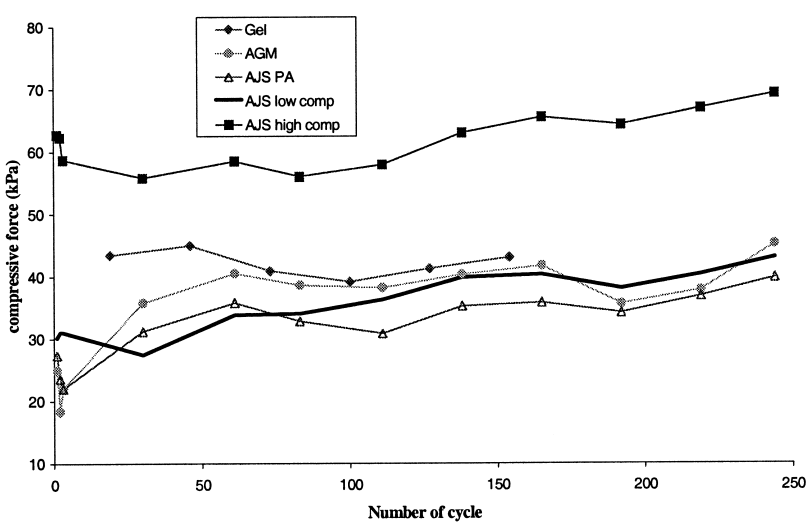

Fig. 8. Dependence of the evolution of compressive forces on cycle number for different separation systems and initial compression.

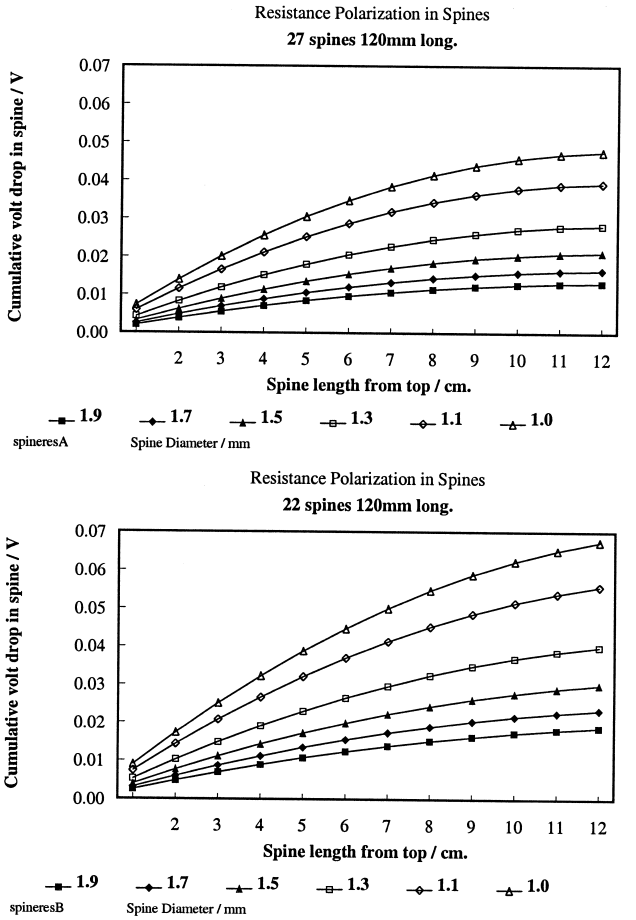

Fig. 9. Voltage drop in spines at 75 A per plate — influences of spine number and spine diameter.

mercial evolution design. The performance of the positive active-material will be improved, subject to electrolyte availability, by the reduction of the active-material thickness, which follows from reduction in plate thickness. Further gains will be achieved by reducing the active-material density. Whilst these improvements are characterised for thicker plates at lower rates of discharge, it is necessary to measure the benefits under the conditions of the DST or ECE-15L driving schedules.

The effect of decreasing the spine mass by reducing the spine diameter or the number of spines on gamma and resistance polarisation have been reviewed. By way of example, Fig. 9 illustrates the influence on the voltage drop (peak current) in spines when the number of spines and their diameter are reduced.

Fig. 10 illustrates how spine resistance, PAM/spine surface area and gamma (g cm^{-2}), are influenced, relative to 27 spines of 1.9 mm diameter, when the spine mass is reduced. Indications are that the adverse effect of reducing gamma is less for mass savings through reduction in diameter than through decreasing the number of spines. Taking advantage of an improved alloy, the influence on gamma will be reduced in both approaches by adopting an elliptical spine section. Further savings arise from reducing and profiling the top bar section according to the calculated voltage drop for the DST or the ECE-15L test.

Replacement of the tube top closure (called ‘carrots’) and part of the lead alloy casting with plastic was considered, but such an approach may be vulnerable to crevice corrosion. The mass and volume of the carrots has been reduced in initial designs; but later it should be possible to adopt any approach successfully demonstrated by CLEPS or Yuasa-Exide.

Whilst the mass of the plastic bottom bar is small, its height creates a penalty in utilising electrolyte and the negative plate, which is below the positive active-material.

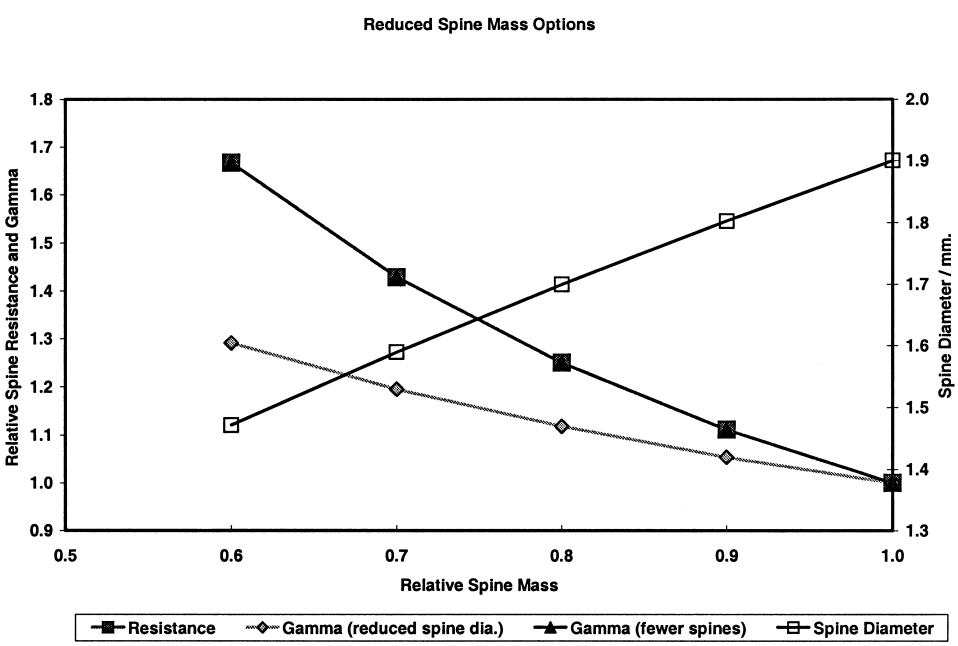

Fig. 10. Spine resistance and PAM (g)/spine surface area influences reduction in spine mass by diameter or by number.

New approaches to reducing this dead height will be pursued during the design revision phase.

In addition to improved formulation/balance, identified in a matrix test, negative-plate performance may be improved by reduction in grid mass. Approaches include the use of thin grids and large pellets (50% of grid mass is in the mesh). Discharged NAM should support large pellets, especially with good separator support, but this approach may not be appropriate if the NAM structure degrades with EV cycles. Negative plates with large pellets are included in the preliminary negative formulation study and the influence of reduced PAM density will be tested in thin-plate cells.

In recognition of the possible requirement to test under either the ECE15L or the DST schedules, the project approach has been adjusted. Instead of evaluating degrees of increasing plate utilisation through reductions of relative spine mass, it has been decided to address the higher power requirement by making a further reduction in plate pitch in order to lower cell impedance.

Adopting a generic design approach, the conflict between battery size restriction, imposed by the available power of the test circuit, and the better performance of larger batteries has been addressed. Test data of relatively low-capacity cells will be used to estimate accurately the performance of larger cells using higher multiples of the same plates. The initial designs are within the test capacity at CMP, to both specifications, and at ZSW for the ECE-15L test. The designs provide, subject to negative grid tool alteration, the option to produce a smaller battery in a different container if it is decided that cycle testing at ZSW should be to DST.

With the exception of the positive plates, component processing was not expected to present any problem. Although negative plates are thin compared with those in existing motive power products, their dimensions are typical of those in other lead–acid product ranges. The tubular positive plates are, however, substantially thinner than those used in existing products. Thin, rectangular-tubed gauntlets, conforming to drawing, were manufactured and delivered on schedule. Injection moulded bottom bars were also manufactured without problem.

Pressure die-cast spine dimensions were thinner than the minimum recommended by the manufacturer of the casting machine and dies. Good quality castings were produced, in lead–calcium–tin (1.2 wt.%) alloy, without any great difficulty. For the initial production, handling was facilitated by hanging the untrimmed castings overnight before cropping and threading the spines into the gauntlets.

Plates were filled with positive active-material precursor using a filter-fill process. In this process, an aqueous suspension is injected, at pressure, and filtered through the gauntlet fabric. Plate thickening through distortion (inflation) of the rectangular tubes was anticipated as a potential problem. Accordingly, expansion control was sought through the addition of a perforated restraining mesh to the filling module.

State-of-the-art test cells with different negative paste formulations, some with large-pellet negative grids, have been made and tested. Declining performance was limited by positive plate polarisation and was not influenced by the controlled variables. Plates have been processed for testing a matrix of design and process variables for thin and extra-thin designs. Some cells have been built and the programme of testing has started. Testing and review of data will be followed by design optimisation during the remainder of the second year.

Better performance under EV duty is expected to arise from the successful development of plates, which are thinner than had been envisaged at the start of the programme. Spine mass reduction has, in one design, been achieved by increasing the aspect ratio of tube sections and using fewer spines. An elliptical section has been adopted for thin spines in order to give increased surface area, which is believed to favour the maintenance of a high conductive interconnection with the active mass. If successfully demonstrated, further mass-saving strategies may be adopted in the revised spine and grid design.

It can be concluded that components, reflecting a substantial reduction in plate thickness in comparison with the state-of-the-art, have been satisfactorily processed in pro-

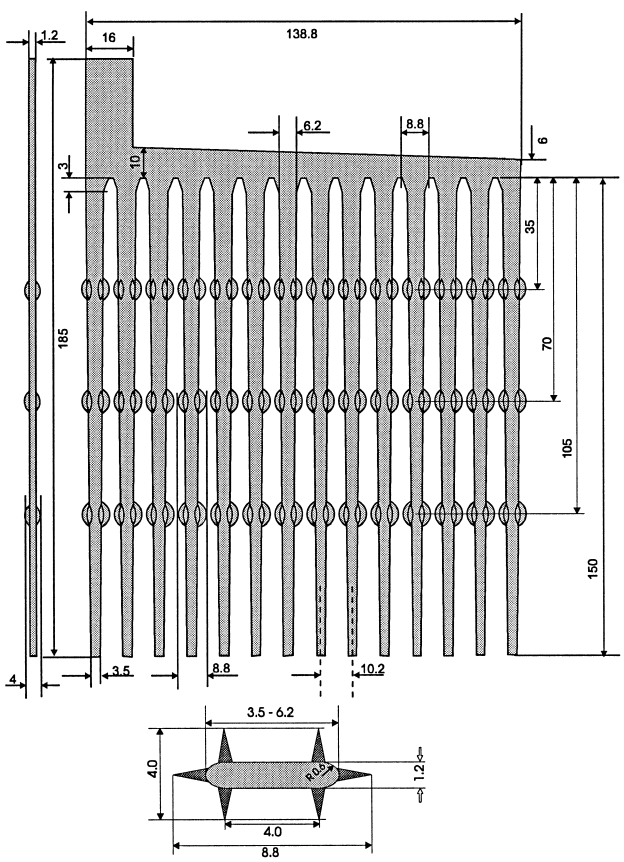

Fig. 11. Optimised cast strap grid design.

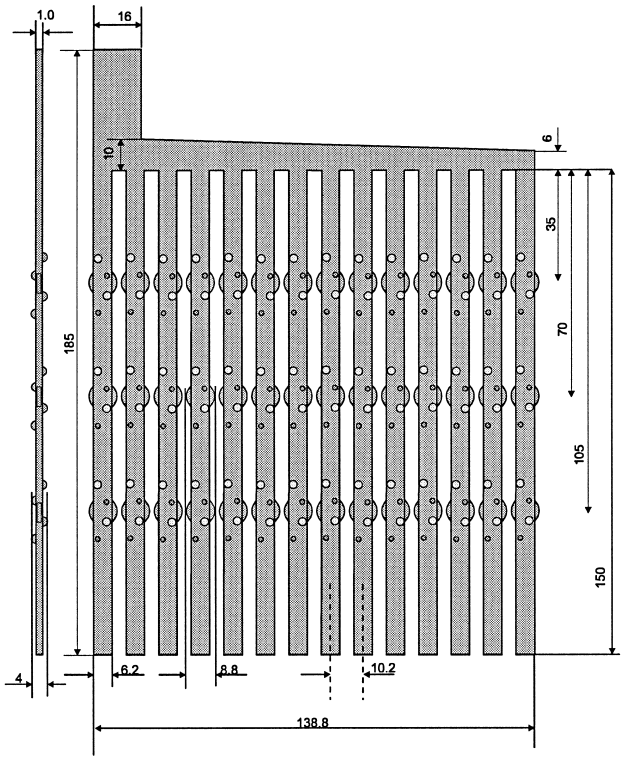

Fig. 12. New die-cut strap grid design.

duction-scale quantities. Test cells using these components have exhibited the designed initial capacities, representing a 50% improvement in specific energy over current designs.

The basic objective of the CLEPS work within task 2(a) is to improve the specific energy and power output of strap grid, tubular plate (SGTP) batteries. This is to be achieved both by optimisation of the SGTP design and, also, by improvement of the utilisation of the PAM through optimisation of the process variables, e.g., filling pressure, phase composition of the paste, and tube fabric.

A new strap grid design for cast grids has been developed with a thickness of 1.2 mm. This is illustrated in Fig. 11. As a result of this, the amount of lead used for casting the grid has been reduced by 19% as compared with the original SGTP design, developed within ALABC Project AMC-004. This reduction in the amount of lead, and hence in grid weight, has been achieved by reducing the thickness of the collector, which interconnects the straps and by changing the form of the straps from rectangular to trapezium-shaped. A mould for the casting of the novel strap grids (with reduced grid weight) has been designed and fabricated at the Institute of Machine Building (Sofia, Bulgaria). Three thousand strap grids were cast from low-antimony alloy in the battery plant of START in the town of Dobrich.

A new strap grid design for die-cut grids has also been developed by CLEPS. In this design, the amount of lead in the die-cut strap grid is reduced by 32% as compared with the original SGTP configuration. A device for the die cutting of strap grids from a lead alloy sheet has been constructed at the Institute of Metal Science of the Bulgarian Academy of Sciences, Sofia. SGT plates were produced with grids die-cut from a lead–calcium–tin strip (180-mm wide) supplied to CLEPS by Cominco, Canada; the design is illustrated in Fig. 12. The important parameters of the two new designs in comparison with the original SGTP design are listed in Table 5.

A mould for injection moulding of the upper plastic covers was designed and constructed in the Institute of Metal Science. A batch of plastic covers was produced. A mould was produced for injection moulding of the plastic strap to plug the tubular plates when filled with suspension. The nozzles of the filling machine were re-designed and the optimised nozzles were produced in the mechanical workshop at CLEPS. A batch of strap grid tubular plates was manufactured employing different filling pressures. These plates were assembled into SGTP batteries, which have subsequently been subjected to testing and an optimum filling pressure has been determined. The way in which the change in filling pressure affects the amount of PAM in the grid and its density is shown in Fig. 13. The variation of plate capacity with plate density and cycle-life with PAM density is shown in Figs. 14 and 15, respectively.

Table 5
Comparative data for the three SGTP designs developed at CLEPS

Parameter	SGTP	New cast SGTP	Change (%)	New cut SGTP	Change (%)
Positive plate height (cm)	13.2	13.2		13.2	
Positive plate width (cm)	14.8	14.8		14.8	
Positive plate thickness (cm)	0.5	0.5		0.5	
Positive grid weight (g)	198	160 ± 5	−19	135 ± 5	−32
Positive plate volume (ml)	58.0	58.0		58.0	
PAM weight (g)	170	180 to 230	+6 to +35	185 to 235	+9 to +38
PAM/(+) Grid weight ratio	0.86	1.13 to 1.44	+32 to +67	1.37 to 1.74	+59 to +102
Positive plate weight (g)	368	340 to 390	8 to +6	320 to 370	13 to +1
PAM utilisation (g/A h)	9.20	9.20		9.20	
A h capacity (A h)	18.5	19.6 to 25.8	+6 to +39	20.1 to 26.3	+9 to +42
γ (g PAM/cm^2 grid)	0.61	0.67 to 0.85	+10 to +39	0.72 to 0.87	+18 to +42

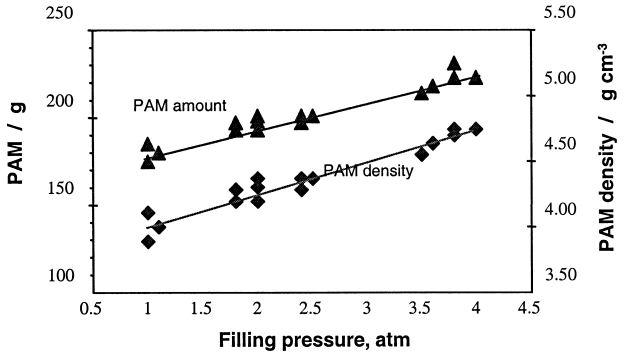

Fig. 13. Dependence of PAM amount and density on filling pressure.

Batches of SGTP batteries have now been manufactured with die-cut and cast strap grids. These have been filled with the active-material suspension by applying a filling pressure of ~200 kPa. These plates have been assembled into batteries and are being cycled.

3.4. Task 2(b): Influence of pulse charge currents on specific energy, life and charging time of advanced tubular EV battery designs

The main objectives of the task are:

1. To enhance the cycle-life of the lead–acid batteries, especially those with thin tubular plate batteries using novel pulse charge algorithms, by:
   - prevention of premature capacity loss of positive active-material by controlling the structure of the active mass and the corrosion layer;
   - prevention of sulphation while deep cycling.
2. To enhance the specific energy of lead–acid batteries by better utilisation of the active mass arising from use of these novel pulse charge algorithms.
3. To increase the fast charge ability of lead–acid batteries by limiting oxygen and hydrogen evolution, and therefore decrease temperature rise and mechanical stress, through novel pulse charge algorithms.
4. To develop a strategy to counter the variation of cell voltages, which is always a problem in battery strings.

Model, low-capacity cells (12 A h, $C_5/5$) with a tubular design of the positive electrode, designed and manufactured at CMP, have been used for the investigation of fast and pulse charge in comparison with a pasted grid design. These were based on cut-down conventional tubular plate designs pending availability of the advanced designs being developed in task 2(a). The design of these cells is given in Fig. 16. Each cell has a built-in reference electrode. The principal parameters of the cells are listed in Table 6. The objective of the task is the investigation of fast and pulse charge for batteries with tubular (conventional and advanced) positive plates. In order to evaluate the results, however, comparative measurements have been done on Hawker Genesis cells (16 A h) with flat plate positive grid electrodes, which is a more favourable design for fast charging.

The measured capacity at the $C_5/5$ discharge rate was 16 and 12 A h for the Genesis and the CMP cells, respectively. The relative capacity vs. discharge rate curves for both cells are given in Fig. 17. As expected, the capacity of the tubular cell design (CMP) is more sensitive to the discharge current than the grid design (Genesis), because of the lower utilisation of the active material and the prolonged diffusion pathways caused by the geometry in the positive tubular electrodes of conventional design. The prolonged diffusion pathways cause an impoverishment of acid within the pores as acid transport into the pores is hindered. The capacity of the model cells at the

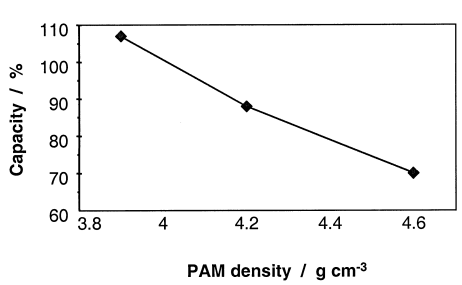

Fig. 14. Dependence of plate capacity on PAM density.

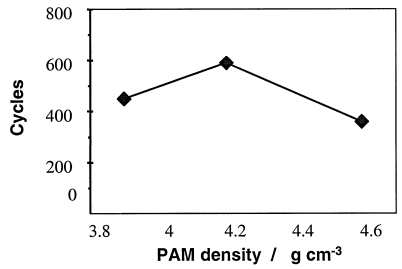

Fig. 15. Dependence of cycle-life on PAM density.

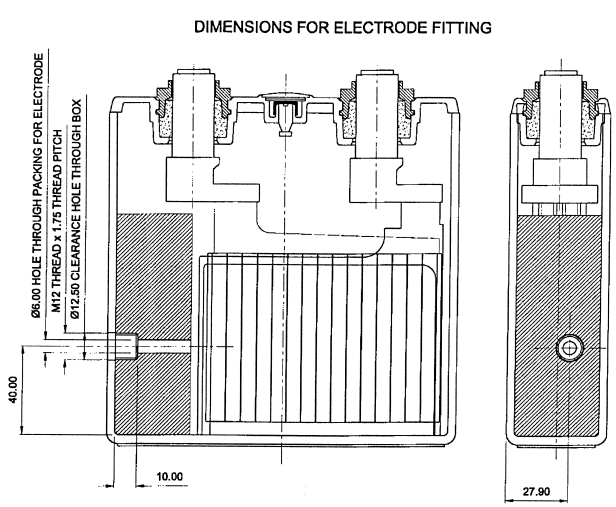

Fig. 16. Design of low-capacity tubular cell.

Table 6
Cell parameters

Positive	Plates	Negative	Plates
Number per cell	2	Number per cell	3
Height (mm)	89.1	Height (mm)	80.7
Width (mm)	102	Width (mm)	110
Thickness (mm)	5.45	Thickness (mm)	2.65
Tube (15) internal (mm)	5.8×4.65	Vertical wires	5
Spine diameter (mm)	2.15	Horizontal wires	9
PAM (g)	101	NAM (g)	70

$C_5/5$ rate was 12 A h and falls to about 60% at the $C_1/1$ discharge rate.

By comparison with the flat plates of the Genesis battery, it was found that limited charge-acceptance of the tubular plate batteries is the main hindrance for fast charging, as can be seen from Fig. 18. The charge-acceptance is defined mainly as the intensity of current, which can be accepted by the battery during the constant current (pulsed) period within the given voltage limit. In general, the higher the initial charge current, the shorter the constant current phase. There are significant differences, however, between the two types of batteries. While the Genesis cell can be charged up to about the 10C rate with a sufficient duration of the constant current period, the CMP cell already has a rather short constant current charge period at the 2C charge rate. The lower charge acceptance of the tubular plate design is not related to a higher internal ohmic resistance, because every charge was carried out with IR-compensated voltage control.

In order to determine the cycling behaviour under different charge regimes, the cells were cycled in groups (each consisted of two series-connected cells) under the following conditions.

Discharge: $C_1/1$ rate (12 A) to a cut-off voltage of 1.6 V, 5 min rest before charge. Discharge at the $C_1/1$ rate means that during discharge about 60% (on average) of the active mass is converted to the discharge product compared with the $C_5/5$ rate and this should not cause any problem for cycling, which could be related to deep discharge. At high discharge rates, however, the conversion of the active mass is not homogeneous, which means that parts of the active mass may be heavily transformed (i.e., deep discharged) to lead sulphate at high polarisation while other parts are hardly transformed.

Charge: For $C_5/5$ charge, the charge voltage was limited every time to 2.35 V (not IR-compensated) and the total duration was 8 h. For the $C_1/1$ or 4C rate, the charge voltage limitation was 2.35 V (not IR-compensated) and the total duration was 2 h. For 4C pulse charge (50% duty cycle), the voltage was limited to 2.4 V (IR-compensated) and the duration was 2 h. Independent of the charge rate, the rest time after charge was limited to 15 min before starting the following discharge. With an increasing number of cycles, the charge current for higher rates becomes limited to lower values at the beginning of charge. Later on, the charge voltage limitation was increased to 2.4 V (for the C rate at cycle 100 and for the 4C rate at cycle 90) and to 2.45 V (for the C rate at cycle 120 and for the 4C rate at cycle 130).

Capacity check. Every 50 cycles, two capacity checks were carried out at the $C_5/5$ discharge rate followed by a charge ($C_5/5$, 2.35 V, 8 h). The development of the capacity is shown in Fig. 19. While the $C_1/1$ capacity for the cells charged at the $C_5/5$ rate decreases only slightly with increasing number of cycles, a rather early decrease in capacity was observed for the charge rates C and 4C, and was even faster for the 4C pulse charge.

Rest times and capacity checks lead to an improvement of the capacity within the following few cycles for the cells charged at the 1C, 4C and 4C pulse rates. For example, the rest time during cycling for the cells charged at the 1C rate was 2.5, 40, 12 and 27 h after 110, 130, 150 and 180 cycles, respectively. This indicates that the low capacity measured during cycling is not only related to the high charge rate but also to the short rest time of 15 min between charge and discharge. When considering fast charge, however, there are only limited applications where high charge rates are needed and there would be time afterwards for the battery to rest.

The charge factor for cells charged at C and 4C was in the range of 1.05–1.07 and seems to be sufficiently high to prevent a loss of capacity by under-charging. For the $C_5/5$ charge rate, the charge factor was about 1.1 (up to cycle number 70) but later fell from 1.07 to 1.04.

Surprisingly, in contrast to the $C_1/1$ capacity during cycling, the $C_5/5$ capacity following the capacity check did not differ so much for the cells charged at different rates during cycling. It is concluded from the behaviour during the capacity check that the high charge rates do not damage the structure of the active mass. Nevertheless, it

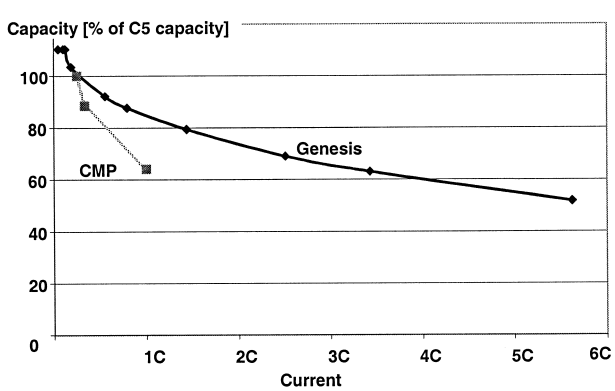

Fig. 17. Discharge capacity depending on discharge current for CMP tubular model cells and the Genesis EP series batteries.

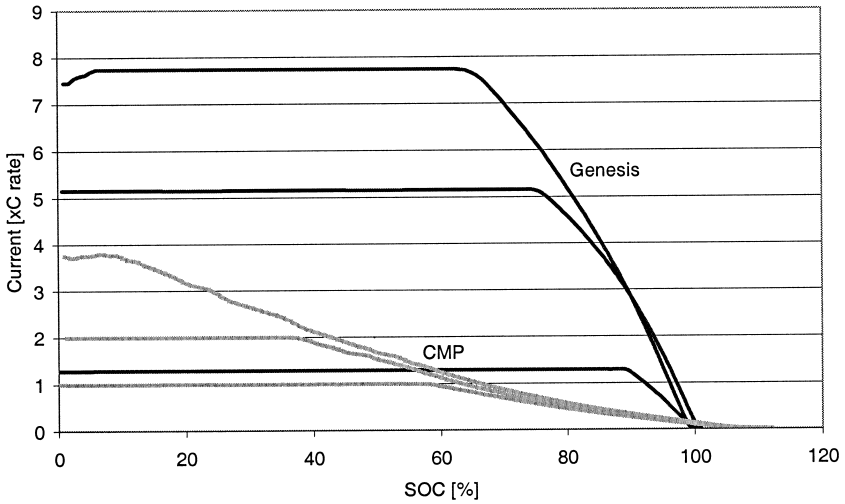

Fig. 18. Charge-acceptance of CMP and Genesis batteries for different charge currents (constant-current charging).

appears that something must have changed in that, during higher discharge rates, only certain parts of the active mass are able to discharge. This phenomenon is probably related to the acid distribution in the electrode.

From the fundamental investigations that have been carried out, the following conclusions can be drawn:

- IR-compensated charge procedures are suitable for controlling the fast charging of lead–acid batteries and allow higher initial charge currents, and an elongation of the constant-current charge period, which results in a reduction of charge time.
- Investigations of pulse charging produce evidence that it is possible to reduce overcharge processes like gassing.
- Pulse charging leads to increased polarisation of the positive and negative electrodes during a current-controlled charge period.
- Both fast charging, as well as pulse charging at high charge rates combined with short rest periods between charge and discharge, lead to a faster decrease in capacity at high discharge rates but do not decrease the capacity for lower discharge rates.
- Analysis of the electrodes did not provide any clear reason for the rather rapid decrease of the high-rate capacity for cells charged at higher rates.
- The conventional tubular design is much less favourable for fast charging, compared with the flat-plate grid design, and is more sensitive to pulse charge (lower charge-acceptance). Therefore, it is necessary to de-

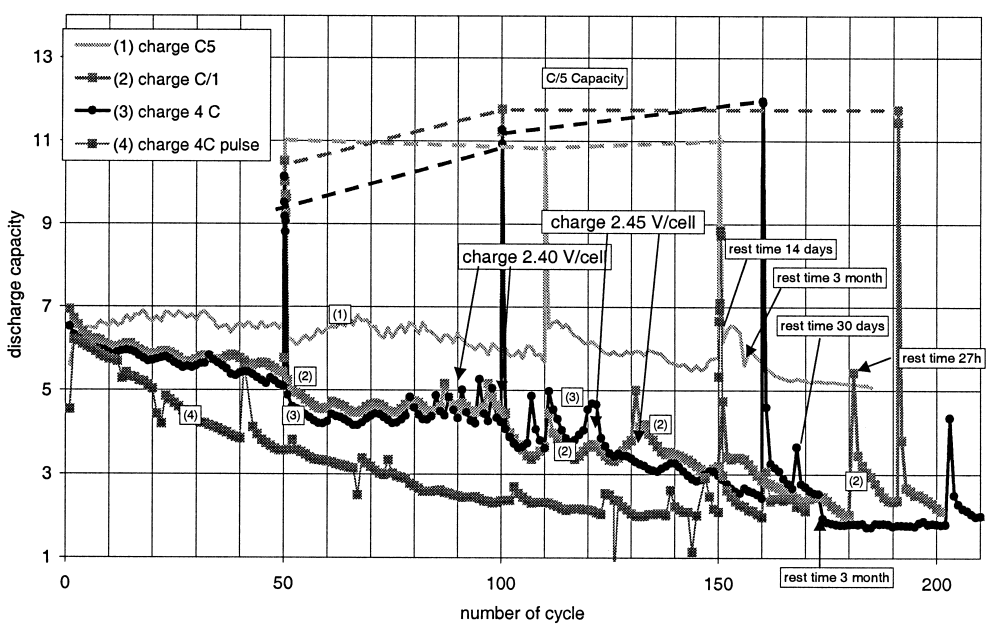

Fig. 19. Development of $C_1/1$ discharge capacity and $C_5/5$ capacity check of 12-A h CMP model cells during cycling at different charge rates.

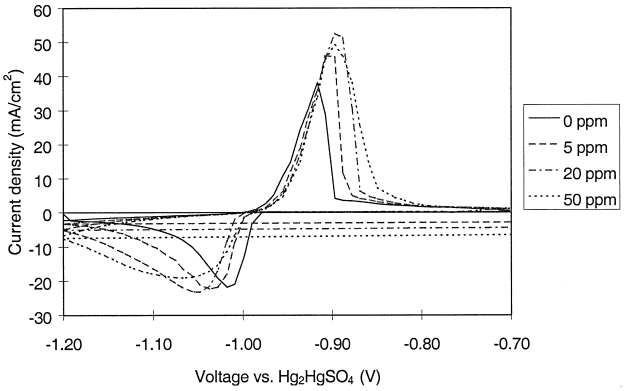

Fig. 20. Voltammogram for Vanisperse A at different concentration levels.

velop an advanced tubular design, which is suitable for fast charge.

Digatron has designed a pulse-charge unit (1500 A/20 V), which was delivered to ZSW at the end of March 1999. Characterisation of the technical parameters has been carried out and the equipment will be used in further investigations. In addition, CMP has now made cells of the advanced tubular design by employing the results obtained in task 2(a). Six cells were delivered to ZSW at the end of April 1999. It should be noted, however, that these cells have not yet been optimised for performance.

3.5. Task 3: Improvement in negative plate performance

The main objectives of this task are as follows.

- Elucidation of the nature of the phenomena leading to degradation of the structure of the NAM as dictated by the mode of battery operation.
- Determination of the influence of the expander on the degradation of the NAM structure.
- Thorough characterisation of the expander materials, using advanced electrochemical and analytical techniques, so that it will be possible to follow the changes in activity under different working conditions.
- Assessment in electrical tests of the characteristics and performance of the NAM, first in plate-group assemblies and then in batteries.
- Develop an optimised expander formulation for the negative plates of VRLA batteries for EV applications.

During the first year, a literature review was carried out. This was aimed at identifying possible expander candidates from different origins, as well as their most meaningful characterisation techniques. From this review, a total of 19 potential expander candidates were selected, viz.,

- conventional expander materials (Vanisperse A, Indulin AT, Kraftplex, Kraftperse DD5 and DD8, N17, NBNa, S-004)
- synthetic materials (B-75, P-63, Diwatex, EZE-Skitan, Darvan 1), vegetable extracts (humic acid, quebracho, mimosa)
- new experimental products from expander manufacturers (UP298, UP393, UP414).

The review of the characterisation techniques led to the conclusion that the most meaningful procedures were those aimed at evaluating the electrochemical activity of the expanders, as well as their chemical composition. Consequently, the techniques of cyclic voltammetry, electrochemical impedance and transient experiments were se-

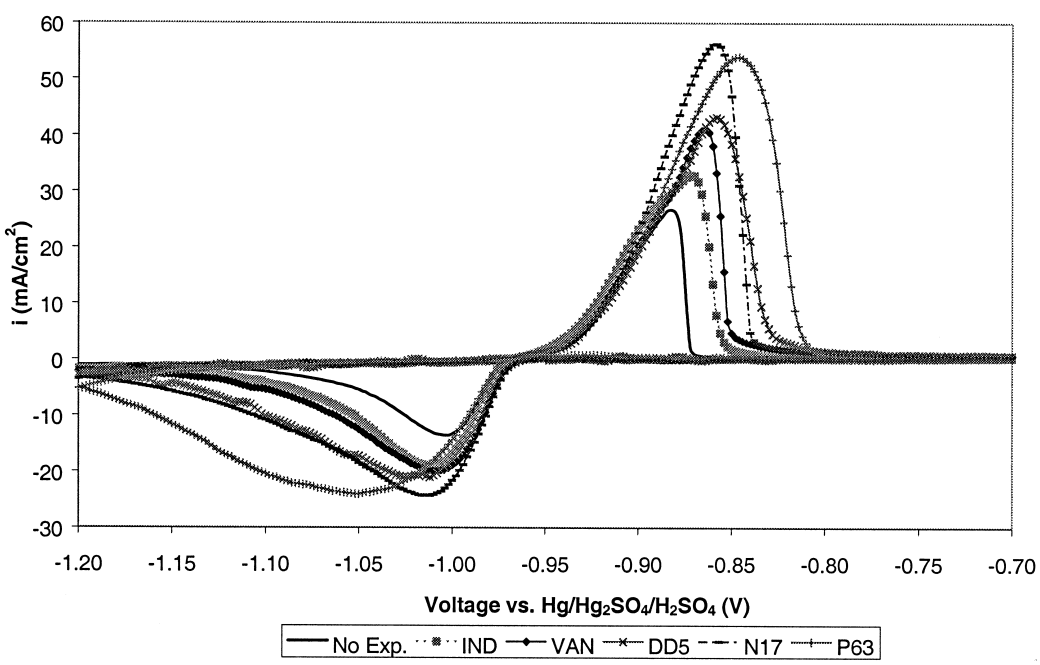

Fig. 21. Voltammograms of most representative expanders.

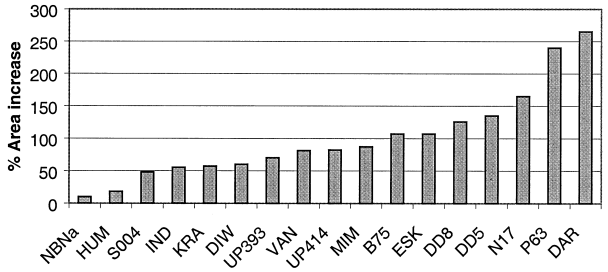

Fig. 22. Increase in anodic peak area for different expanders — expander efficiency.

lected in addition to chemical characterisation using analytical procedures. The task partners agreed that cyclic voltammetry would be carried out at the Tudor Research Laboratory in Spain (Tudor), while the remaining tests would be carried out at the Politechnical University of Turin in Italy (POLITO).

The tests carried out by Tudor employed an electrochemical cell (100 cm^2), which consisted of a working electrode made from pure lead (a rod of approximately 15 mm length and 5 mm diameter), a counter-electrode also made of pure lead and a $Hg/Hg_2SO_4/H_2SO_4$ reference electrode. All potentials are reported with respect to this reference electrode. The tests involved execution of a series of cyclic voltage scans in the working voltage range of the negative electrode (-1200 to -700 mV) in the presence of the respective expander dissolved in the electrolyte. Thus, the electrode was 'formed' by a continuous series of charge–discharge cycles with the respective expander, until a constant voltammogram was found. Also, blank tests were performed in an electrolyte without expander. These blank tests were carried out periodically, in order to take into account any eventual degradation of the lead electrode.

A typical voltammogram for Vanisperse A is shown in Fig. 20. From the tests done on the different expanders, it can be observed that, although the general behaviour of all the candidate expanders is similar, nevertheless, quite large differences can be found among them, and between them and the voltammogram obtained in absence of expander. In all cases, the presence of expander increases the anodic peak area (i.e., the discharge capacity), but also modifies the cathodic peak voltage (i.e., the charge-acceptance behaviour). Therefore, all the expanders tested modify, to a greater or lesser extent, both the charging and discharging behaviour of the lead electrode. This can be observed in Fig. 21, where some of the most representative expanders tested are compared.

In the absence of expander, both the anodic and the cathodic peaks are small, but well defined. All the expanders produce an increase in the voltammetric area, and also a larger or smaller tail in the cathodic peak. In the extreme case, expander P-63 produces very large peaks but also a very distorted cathodic peak. This indicates a high efficiency but also a very high inhibition of chargeability. Therefore, the extent to which each expander modifies the electrode performance is quite different, as it can be observed in Fig. 22. Here, the different increases in anodic area are represented in respect to the voltammogram obtained with pure acid.

The increments in peak area obtained for the different expanders ranged from around 10% for the NBNa, to more than 250% for DAR. Therefore, very high differences can be found in this test for the different expanders investigated. This suggests that a ranking of expander efficiency of the candidates could be as follows:

(1) Low area increase (up to 60%)	NBNa, HUM, S-004, IND, KRA,DIW,VAN,MIM,B75,E-SK
(2) Intermediate area increase (60 to 120%)	DD8, DD5, N17
(3) High area increase (120% to 180%)	P-63, DAR
(4) Extremely high area increase (more than 180%)	

On the other hand, the polarisation values, which are indicators of the charge-acceptance behaviour of the electrode, are represented in Fig. 23. Again, some differences have been found among the different expanders tested, although not as large as in the previous parameter (except for DAR and P-63). An approximate classification of the values obtained is:

(1) Extremely high polarisation (more than 20 mV)	DAR, P-63
(2) Intermediate polarisation (10 to 20 mV)	E-SK, DD8, B75, KRA, DD5
(3) Low polarisation (less than 10 mV)	N17, MIM, IND, VAN, DIW, HUM, NBNa, S-004

Unfortunately, the expanders, which produced the best efficiency, show also an extremely high polarisation (DAR,

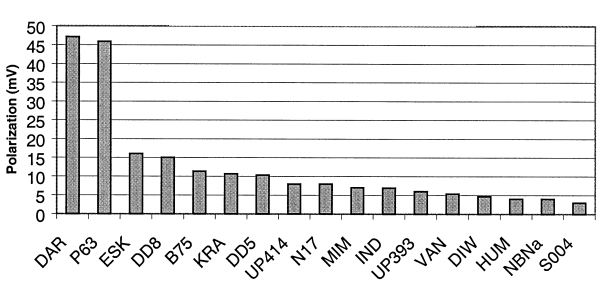

Fig. 23. Cathodic peak polarisation for different expanders — charge inhibition.

Table 7

Performance	Expander
HIGH (high efficiency, intermediate to low polarisation)	N17, DD5, DD8
INTERMEDIATE (intermediate efficiency, intermediate to low polarisation)	B75, ES-K, VAN, MIM
LOW (low efficiency, intermediate to low polarisation)	DIW, KRA, IND, S-004, HUM, NBNa
SPECIAL CASES (extremely high polarisation)	P-63, DAR

P-63). Therefore, these substances have to be discarded for use as expanders.

Thus, the materials that produce a high increase in area (and therefore a higher capacity in discharge), also produce a higher cathodic peak polarisation, which indicates a worse charge-acceptance performance. This is in good agreement with the previous experience about the behaviour of different expander materials. In the present case, the best candidates from the 'efficiency' test have to be discarded due to their unacceptable polarisation values. Similarly, some of the expanders with very good polarisation values have to be discarded due to their low efficiency.

Taking into account the trade-off between both studied parameters, the final ranking of tested substances regarding the cyclic voltammetry tests can be seen in Table 7.

The first year (1998) of the work programme carried out at the Politecnico di Torino included the following activities.

- Electrochemical testing on flat lead electrodes, including impedance measurements, transient recording, potentiodynamic curves. The most significant tests were performed both in 0.5 and 5 M sulphuric acid.
- A list of 17 different expanders has been considered for testing. All expanders were subjected to chemical and electrochemical characterisation.
- Thermal stability has been checked by keeping the solution containing the expander at 75°C for 1 week. After this treatment, electrochemical testing was performed.
- A first screening for analytical characterisation of the expander materials.

The work programme during the second year involved the following activities.

- Electrochemical testing on small plates or pasted mini-electrodes, including polarisation curves, both potentiostatic and potentiodynamic.
- Measurement of gas evolved on negative plates, previously wetted in sulphuric acid, at open-circuit. These experiments are performed in thermostatically controlled, sealed glass vessels, connected to a pressure measurement device and are aimed at evaluating the different rates for hydrogen evolution, as a consequence of the presence of different expander materials.
- Chemical characterisation of the expanders.

Table 8 ranks the expanders according to the different tests carried out both at POLITO and Tudor.

Taking into account all the characterisation tests, performed both at Tudor and POLITO, and in some cases including a thermal pre-treatment at 75°C during 1 week, a more comprehensive picture of the electrochemical performance of the expanders has been obtained. From the final ranking achieved, the seven most effective additives (according to their electrochemical performance) have been

Table 8
Effectiveness of expanders according to different electrochemical tests

Effectiveness	Impedance measurements	Oxidation transients	Reduction transients	CV tests (Tudor)	Treatment at 75°C
Major effect	NBNa	DD8	Quebracho	Darvan 1	Vanisperse A
	S-004	EZE-Skitan	B-75	P63	Diwatex
	Darvan 1	N-17	Diwatex	N17	S-004
	B-75	S-004	N17	DD5	EZE-Skitan
	DD8	DD5	Mimosa	DD8	N17
	Mimosa	Darvan 1	Vanisperse A		Mimosa
	Quebracho	Quebracho	Indulin		Kraftplex
Relevant effect	EZE-Skitan	Vanisperse A	UP298	B-75	NBNa
	Vanisperse A	Kraftplex	EZE-Skitan	EZE-Skitan	DD8
	Kraftplex	P-63	DD5	Mimosa	Quebracho
	P-63	Humic acid	DD8	Vanisperse A	UP289
	Humic acid	B-75	NBNa	Diwatex	DD5
	DD5	Diwatex	Humic acid	Kraftplex	B-75
		UP298	S-004	Indulin	Darvan 1
Low effect	Indulin AT	Indulin AT	Kraftplex	S-004	Humic acid
	Diwatex	NBNa	P-63	Humic acid	Indulin AT
		Mimosa	Darvan 1	NBNa	P-63

selected for further testing in VRLA cells. These additives are: N17, DD8, DD5, S-004, Vanisperse A, Kraftplex and UP414.

To date, all the activities in relation to the manufacturing process of VRLA cells have been completed. Furthermore, different formulations have been defined, including each of the previously selected expanders, as well as several additional experiments with different concentrations of the expander, carbon black or barium sulphate for the most promising candidates.

The first seven mixing/pasting/curing experiments have been conducted. These include each one of the selected expander candidates at the same concentration and with the same amounts of carbon black and barium sulphate. Samples of the resulting negative plates have been sent to POLITO for characterisation tests with pasted mini-electrodes. Next, the remainder of the formulations will be produced, and the cells will be assembled, formed and electrically tested for their initial performance and cycle-life.

The basic objectives of the work in task 3, which is being carried out at CLEPS are:

- to investigate the nature of the phenomena leading to degradation of the structure of the NAM and hence the performance of the negative plate,
- to determine the optimum proportion between the two types of NAM structures, and
- to investigate the influence of expanders on the degradation of the NAM structure.

Batches of negative pastes were produced with Indulin, and a mixture of Indulin and Vanisperse, as expanders. The negative grids (motorcycle type) were pasted and batteries with these plates were assembled. These batteries were subjected to ECE-15L cycling tests.

Batches of negative pastes were produced with Indulin, a mixture of Indulin and Vanisperse, and Kraftplex used as expanders. The negative grids, sent by Tudor, were pasted and batteries with these plates were assembled. Batteries of the Tudor type were subjected to ECE-15L cycling tests. The results provide evidence that the longest cycle-life and the highest capacity for negative plates are obtained when a mixture of Indulin and Vanisperse is used as the expander. The increase in battery temperature during operation leads to an increase in capacity and cycle-life performance of the negative plates.

Scanning electron microscopic studies show that, on ECE-15L cycling, the secondary energetic structure of the NAM is transformed into a skeleton structure. As a result of this conversion, the capacity of the negative plates decreases and they reach their end of life. At higher temperatures, the NAM expands, which is the reason for failure of the negative plates.

Investigations were made of the stability of two expanders (P-63 and Kraftplex) to hydrogen and oxygen attack. The results show that the P-63 expander is not stable under the action of either gas, whereas Kraftplex is stable in a hydrogen medium.

The work of CLEPS in task 3(a) was originally scheduled solely for 1998 and this has been completed successfully. The results obtained are very interesting and they indicate that negative plates prepared with a mixture of two expander products give better performance than conventional ones. Further investigations and battery tests are required to determine the optimum amount of expander to be used, as well as the optimum proportion of the components in the expander blend. Thus, the programme of work has been extended into 1999.

4. Conclusions

The second EALABC Brite-EuRam Project has reached its mid-point and the following conclusions can be drawn from the work completed to date.

- In task 1(a), four new separator variants have been developed and are under cycle testing. Initial results look promising.
- In task 1(b), the new AJS separator is being compared with AGM and gel separators. Again, initial results look promising and the good cycling performance of the initial material has in fact delayed optimisation work on the separator.
- In task 2(a), work at CMP Batteries and CLEPS has demonstrated that it is possible to make substantial weight reductions from previously established practice in conventional and strap grid tubular designs. Improved specific energies are being recorded and optimisation and life-cycling of these designs will take place during the next phase of the Project.
- In task 2(b), from the work performed to date, it would appear that conventional tubular batteries are less suitable for pulse and fast charging than advanced flat plate designs. During the second phase of the Project, advanced tubular designs will be evaluated under several different charging regimes in conjunction with ECE-15L discharge cycles.
- In task 3, methods have been used to evaluate expander materials in laboratory conditions and rank them according to overall efficiency. These expanders are now being incorporated into batteries in order to assess the validity of these results in battery operation. Additionally, it would appear that a mixture of two expanders could perform better than either of the two components individually. Further work in this area is being carried out to see if these benefits can be predicted and optimised for mixtures of different materials.

In general, it is considered that the Brite-EuRam Project has made a promising start and additional work has been agreed in some areas. In addition, some preliminary work

is being done on evaluating the possible use of a microporous ceramic material as a separator.

Acknowledgements

This work has been sponsored jointly by the European members of the Advanced Lead–Acid Battery Consortium and the European Commission under the Brite-EuRam Programme. Their permission to publish this paper is gratefully acknowledged. This summary of the work to date has been produced from Progress Reports produced by the various researchers for the Project Mid-term Report.

References

[1] E. Valeriote, Rapid charging of electric vehicle batteries, in: ALABC Members and Contractors Conference, London, 1995, February.
[2] L.T. Lam, O.V. Lim, H. Ozgun, C.G. Phyland, D.A.J. Rand, D.G. Vella, L.H. Vu, N.C. Wilson, ALABC Project RMC-008, Pulsed-current charging techniques for lead/acid electric-vehicle batteries, Final Report: January–March 1997, April 1997, 79 pp.
[3] A. Cooper, J. Power Sources 59 (1996) 161–170.